

PROGRESS REPORT NO. 1

MECHANISM OF THE PHOTOVOLTAIC EFFECT IN II-VI COMPOUNDS

National Aeronautics and Space Administration  
Lewis Research Center  
Cleveland, Ohio

April 1 - September 30, 1967

School of Engineering  
Department of Materials Science  
Stanford University  
Stanford, California

Grant NGR-05-020-214

Principal Investigator

Richard H. Bube, Professor

Report Prepared by:

R.H. Bube  
W. Gill  
P. Lindquist

## INTRODUCTION

The purpose of this project is to formulate and perform a series of experiments which will help to establish the mechanism of the photovoltaic effect in heterojunctions consisting of a II-VI compound and a metallic or quasi-metallic barrier layer. In particular, attention is focused on the mechanism of the CdS:Cu cell which is now being fabricated commercially and which has potential advantages over the silicon photo-cells now in use in spacecraft.

Whereas the commercial CdS cells utilize thin, polycrystalline layers of CdS, this research is concerned primarily with single crystal material. It is generally found that the thin film cells have superior performance in terms of power output, but for the purposes of a fundamental study it is at least initially desirable to eliminate the complicating effects of crystal boundaries.

Investigators at Clevite Corporation have recently set forth a proposed mechanism for the operation of the CdS:Cu cell.<sup>(1)</sup> This model is not discussed in the present report, but it is expected that the techniques described here will lead to results of general significance with regard to the validity of this or any other model in the future. This report summarizes the materials used, the measurements made, and some of the more interesting results obtained on the program thus far.

## MATERIALS

The following is a listing of the materials used to date:

CdS - (a) Clevite single crystal, oriented with c-axis perpendicular to the plate, low resistivity (1-10 ohm-cm.).

(b) Clevite single crystal, unoriented, intermediate resistivity ( $10^4$  ohm-cm.).

CdSe - Clevite single crystal, oriented with c-axis perpendicular to the plate, low resistivity (1-10 ohm-cm.).

ZnS - Harshaw single crystal, oriented with c-axis in plane of plate, annealed in Zn at Stanford ( $>10^8$  ohm-cm)

CuCl - Baker and Adamson reagent grade (98%)

Cu<sub>2</sub>S - K & K Laboratories, 95-99%.

## PREPARATION OF PHOTOVOLTAIC CELLS

The following techniques and processes have been used to produce photovoltaic cells from the single crystal II-VI compounds.

### (1) Chemical Dipping

(a)  $\text{CuCl}$  solution. Saturated solution of reagent-grade  $\text{CuCl}$  in  $\text{H}_2\text{O}$  (distilled), heated in air in shallow dish on hotplate. Crystal mounted on glass slide with black wax, exposing only the surface to be dipped. Slide immersed in hot solution ( $90^\circ\text{C}$ ) for prescribed time, then rinsed and dried.

(b)  $\text{Cu}_2\text{S}$  solution. Solid  $\text{Cu}_2\text{S}$  dissolved in  $\text{NH}_4\text{OH}$  to form a brilliant blue solution. Same dipping technique as above.

Note: All chemical dipping during this report period has been done in air.

### (2) Plating

Thin layers of copper metal were plated on to CdS crystals using a standard cyanide bath. Compositions of the plating solution per 100 cc water was 2.2g  $\text{CuCN}$ , 2.6 g  $\text{NaCN}$  and 0.74 g  $\text{NaCO}_3$ . The anode was 0.994 copper sheet. Plating current density was approximately  $1 \text{ ma/cm}^2$ .

### (3) Heat Treatment of Photovoltaic Cells

The technique most frequently used has been to heat treat the diodes for 10 minutes in air at  $250^\circ\text{C}$ . The diode is placed in an open-ended quartz tube which is inserted into a small tube furnace.

### (4) Surface Preparations

The following surface treatments have been used in preparing the II-VI crystals for the formation of the barrier layer.

- (a) Crystal surface as received.
- (b) Etched in concentrated HCl.
- (c) Abraded with fine emery paper.
- (d) Polished with 1 micron alumina on silk.
- (e) Ground with 5 micron alumina on glass plate (produced "frosted" surface which approximates the as-received surfaces of the oriented Clevite CdS and CdSe crystals).
- (f) Cleaved.

(5) Ohmic Contacts

Two adjacent indium dots, each about 0.5 mm in diameter and separated by about 1 mm, are evaporated on both the Cu side and the II-VI side near one end of the crystal. The contacts are checked electrically by measuring the V-I characteristic between the pairs of dots, on each side of the crystal. Light etching in HCl was found to promote good Ohmic contact to the II-VI side. Fine copper wires are attached to the indium dots by means of conducting silver paste.

MEASUREMENTS

(1) Spectral Response

The spectral response of the photodiodes was measured using a Bausch and Lomb Grating Monochromator (Model 45-01) with a tungsten light source. A small optical bench was mounted rigidly to the front end of the monochromator to allow accurate and reproducible positioning of the specimens. A small lens mounted in front of the crystal specimen serves to focus the output beam from the monochromator, and a movable mask in front of the crystal was used to limit the area of illumination and to shield the contacts from the light. For measurements involving

a second "bias" illumination, a PEK Lab high-pressure xenon source was used. The beam from the xenon source passes through a beam splitter and thus illuminates the crystal at normal incidence, as does the beam from the monochromator. The configuration is shown schematically in Fig. 1. The wavelength of the bias illumination is varied by means of interference filters. The spectral region scanned is from 0.4 to 1.4 microns. The output of the photodiode is recorded on a Keithley 149 Milli-microvoltmeter as the open-circuit photovoltage, or short-circuit photocurrent by measuring the voltage across a small precision resistor in series with the diode. Measurement of the short circuit photocurrent is preferred in order to avoid saturation effects.

(2) V-I Characteristics

The voltage-current characteristics of the photodiodes, in the dark and also under various conditions of illumination, are recorded on Polaroid film with a Tektronix Type 575 Transistor Curve Plotter. The curves can be conveniently measured with the sample mounted in place for spectral response measurements.

(3) Power Output

The power output of the photodiodes is measured by recording the self-generated voltage-current characteristic by means of the circuit shown in Fig. 2. Again, the crystal is mounted in position for spectral response measurements, as in Fig. 1. The "zero" or mirror position of the monochromator is used to obtain the full output of the tungsten source, with neutral density filters to vary the integrated intensity.

#### (4) Capacitance

Early attempts were made to measure the voltage-dependent capacitance of the photodiodes using a General Radio 1608-A Impedance Bridge and an RLC biasing network. These measurements were unsuccessful because of the poor resolution of the bridge and the broad nulls due to the small parallel resistance (low Q) of the specimens. Therefore, a Boonton Model 75D capacitance bridge was purchased. This bridge has a built-in biasing network which can be used with either the internal or an external DC power supply. Another important feature is a detector which can be made insensitive to changes in phase angle, thus permitting rapid and precise balancing of the bridge by means of the capacitance adjustment alone. The three-terminal nature of the capacitance measurement allows the specimen to be some distance away from the bridge, since the capacitance of the lead wires is automatically subtracted out. Therefore the diode can be mounted on the monochromator, and capacitance-voltage curves in the presence of illumination can be measured. The test frequency of the bridge is 1 MHz, which is sufficiently high so that spurious effects due to trapping are absent. An external DC power supply, HP 711a, is used because of its good regulation.

#### (5) X-Ray Diffraction

In addition, to the usual Debye-Scherrer cameras and diffractometers for routine identification, a microfocus X-ray source is available for dislocation topography by the Lang or Bormann methods. The application of topographic studies to the problem of characterizing the junction region of the photodiodes will be investigated during the next report period. During the period just completed, only

orientation and powder-pattern identification measurements have been made.

(6) Electron Diffraction and Microscopy

A Hitachi HU-11 electron microscope with a reflection diffraction stage has been used to obtain diffraction patterns from dipped layers on single crystals of CdS, CdSe, and ZnS. During the next report period, work will be done to develop techniques for studying the structure of the junction regions by transmission microscopy.

(7) Optical Transmission

A Cary 14 double-beam spectrophotometer was used to measure optical transmission of dipped single crystals.

RESULTS

The experiments to date have been oriented toward the development of proper techniques for the measurements described above, and toward the acquisition of preliminary data to establish the magnitudes and ranges of variation of the measured quantities. Some data representative of the kinds of results obtained are presented in this section.

Fig. 3 indicates the optical transmission of a typical CdS-Cu<sub>2</sub>S cell. This cell was produced by dipping three minutes in a 95°C solution of CuCl<sub>2</sub> in water. The band gap of Cu<sub>2</sub>S is at 1.2 eV, and the transmittance falls gradually for shorter wavelengths. The slight structure at 1.5 eV. is probably a multiple reflection effect. 1.8 eV is the energy of the second indirect band gap in Cu<sub>2</sub>S.<sup>(1)</sup>

Figs. 4-6 present data for a cell made by cleaving a conducting (1-10 ohm-cm) CdS crystal on (11 $\bar{2}$ 0) and dipping for one minute in CuCl<sub>2</sub>. The properties of the cell were measured as a function of time of heat treatment at 250°C in air. The cleaved crystal surface reacts



more slowly with the  $\text{CuCl}$  solution than do surfaces prepared by the other methods, and therefore only a very thin layer was formed by the one-minute dip. The cell gave an open-circuit photovoltage of over 0.4 volts with no heat treatment. The table below gives the effect of time at  $250^\circ\text{C}$  in air on the open-circuit photovoltage ( $V_{oc}$ ) in white light and on the capacitance at 1 MHz in the dark, with zero applied bias.

<u>Time at <math>250^\circ\text{C}</math></u>	<u><math>V_{oc}</math> (white)</u>	<u><math>C(V=0)</math> (dark)</u>
0	405 mv	360 pf
2	470	380
7 (2 + 5)	450	640
17 (2 + 5 + 10)	450	670

The sudden increase in capacitance after 7 minutes may be associated with a change in the contacts on the  $\text{Cu}_2\text{S}$  side during heat treatment. However, it is evident that the capacitance does increase with increasing time of heat treatment, contrary to what one would expect if the effect of heat treatment is envisioned as spreading out the junction region.

Fig. 4 shows the results of the power measurements made after 0, 2, 7 and 17 minutes at  $250^\circ\text{C}$ . Using the usual "fill factor" criterion of maximum power output, it is evident that the power goes through a maximum at about 7 minutes. From the above table, and the intercepts on the voltage axis in Fig. 4, it is seen that the open-circuit photovoltage goes through a maximum, also. From Fig. 4, one also sees that the short-circuit current decreases monotonically with time in a roughly exponential fashion.

Fig. 5 is the V-I characteristic of the diode in the dark, after the total 17 minutes at 250°C. The curve changed very little during the successive heat treatments, which indicates that the V-I characteristic is not a sensitive indicator of cell performance.

Fig. 6 gives the frontwall spectral response of the same cell, also after the total 17 minutes of heat treatment at 250°C. The response in the presence of a 9000 Å "bias" light source is also given, the signal due to the bias illumination being zeroed out. The effect of the bias light is relatively small in this example. No effect at all was observed until after 7 minutes at 250°C.

The frontwall spectral response of another conducting CdS cell is given in Fig. 7. In this case a much larger effect of the 9000 Å bias light is evident, the difference being a factor of 4 at 5000 Å. This cell was prepared by grinding the (0001) faces with 5 micron alumina on a glass plate ("frosting"), and dipping for 90 seconds in the CuCl solution after leaving the crystal exposed to the atmosphere for 2 days. A 10 minute heat treatment at 250°C in air was used.

In addition to the conducting crystals of CdS, intermediate resistivity crystals (about  $10^4$  ohm-cm) have also been used to prepare cells. The much higher resistivity of these crystals results in diodes with relatively very wide depletion regions, of the order of 10 microns. Also, it has been found that the surface treatments before dipping have very little effect on the maximum open-circuit photovoltage subsequently obtained, whereas the photovoltage of the conductive CdS cells is quite sensitive to prior surface preparation. In Fig. 8 the V-I characteristics of one of these cells are presented. Notice that the light has

very little effect on the forward characteristic, but that the reverse characteristic shows a "kink" under illumination. This effect has been observed in other cells made from the high-resistivity CdS, under both frontwall and backwall illumination. No complete explanation for this effect has been found to date, but it is thought to be related to photoconductivity processes in the CdS which are not as prominent in the conducting materials. Fig. 9 gives the effect of 9000 Å bias on the spectral response of this cell. The signal produced by the bias light alone was 50 mv. The effect of the bias light in this case was to decrease the photovoltage over the entire spectrum, with a sharp drop to zero at 5000 Å, the bandgap of CdS. This effect must also be related to photoconductivity in the CdS.

Figs. 10-13 give some measured properties of a cell formed from the conductive CdS by dipping an as-received (0001) face in a hot solution of  $\text{Cu}_2\text{S}$  dissolved in  $\text{NH}_4\text{OH}$ . This solution also produces a black layer, but it reacts much more slowly with the CdS than does the  $\text{CuCl}$  solution. The motivation for using the  $\text{Cu}_2\text{S}$  solution was to determine whether any noticeable difference occurred which could be attributed to the absence of the halogen.

Fig. 10 shows the forward current-voltage curve, measured in the dark. The bending-over at higher voltages is found in many heterojunction diodes, and has been interpreted as a transition from diffusion-limited to emission-limited current, and also as being due to tunnelling processes through the narrow potential spike caused by the sudden discontinuity in electron affinity at the interface.

Fig. 11 gives the spectral response of the cell for both front-

wall and backwall configurations. The open-circuit photovoltage in white light from the monochromator with slits set at 2 mm. was only 39 mv (frontwall) and 11.5 mv (backwall). These values were far from the saturation value of  $V_{oc}$ , because with a microscope illuminator focussed directly on the crystal, a photovoltage of about 300 mv was obtained (frontwall). Usually, the CuCl-dipped crystals have been found to be much closer to saturation when illuminated by white light from the monochromator. The form of the spectral response curve is considerably different from that of Fig. 6, in that the plateau region from about 5000-9000 Å is missing. A similar form of spectral response curve was obtained with a high resistivity crystal of CdS dipped in the Cu<sub>2</sub>S solution. It is not yet known whether these variations in spectral response represent a fundamental difference in the structure of the layers produced by the two different solutions. This will be decided by diffraction studies.

The capacitance-voltage curve in the dark is given in Fig. 12. The usual inverse-square relation between capacitance and applied voltage does not hold. The shape of this curve is very reproducible, although the magnitude varies several percent from day to day. Very noticeable transient effects in the capacitance, due to applied reverse bias and also to sudden changes in illumination, were observed. Fig. 13 illustrates the decrease in zero-bias capacitance with time after switching off a source of white light at  $t = 0$ . Fig. 14 shows the increase in capacitance with time when a reverse bias of 1 volt is suddenly applied. The data approximately fit a relation of the form

$$\frac{C_2 - C(t)}{C_2 - C_1} = e^{-t/\tau}$$

where  $C_1$  is the capacitance at  $t = 0$  and  $C_2$  is the value attained after a long time. The data of Fig. 14 were fitted to the above expression after correcting for a small zero drift in the bridge. The result is plotted in Fig. 15, showing that the expression above is fairly well obeyed except for very short times. This transient effect under reverse bias has been recently reported in GaAs: Au diodes, and in that case it has been attributed to either trapping processes in the depletion region or to charge accumulation at surface states in the interface region.<sup>(2)</sup> In the present example, this transient effect was found to reverse itself for voltages greater than 3.5 volts reverse, i.e., the capacitance then decreased with time. A systematic investigation of these transient effects, involving their dependence on temperature, may yield significant information about the electronic processes in the junction region.

The results of some preliminary diffraction studies may also be reported at this time. Fig. 16 is a Debye-Scherrer X-ray film of a portion of a  $\text{Cu}_2\text{S}$  (nominally) layer which flaked off a CdS crystal substrate after a dipping time of 5 minutes in the  $\text{CuCl}$  solution. The tiny flake was not ground up but was mounted whole in the camera. A very noticeable curvature of the flake indicated the presence of internal stresses. This is reflected in the X-ray pattern by the presence of the broad, radial streaks and also by the fact that the d-spacings are shifted from those of ideal  $\text{Cu}_2\text{S}$ . A number of lines are also present in the pattern which do not correspond to  $\text{Cu}_2\text{S}$  even with distorted cell

parameters. The polycrystalline nature of this dipped layer is clear. Shiozawa et al reported epitaxial growth of the  $\text{Cu}_2\text{S}$  on CdS, with the c-axis of the  $\text{Cu}_2\text{S}$  parallel to the c-axis of the CdS.<sup>(1)</sup> Singer and Faeth<sup>(3)</sup> also recently reported the formation of a single crystal of  $\text{Cu}_2\text{S}$  on CdS with an epitaxial relationship after extremely long time (18 hours) in the  $\text{CuCl}$  solution. The X-ray pattern of Fig. 16 indicates preferred orientation of the  $\text{Cu}_2\text{S}$  crystallites by the arcing of the rings, but other orientations of the c-axis relative to the c-axis of the CdS must be involved to produce such a large number of rings.

Fig. 17 presents a single-crystal reflection electron diffraction pattern from a dipped CdS cell. The pattern was indexed consistently as  $\text{Cu}_2\text{S}$  in the  $(2\bar{1}\bar{3})$  orientation, using the published lattice constants. In this case, the CdS substrate was in the (0001) orientation, which shows that the epitaxial relationship of Shiozawa et al, is not always obtained. This diffraction pattern was obtained from only one small portion of the dipped surface; in most places on the surface a pattern of spotty rings was found, indicating a very small crystallite size.

Fig. 18 demonstrates that the dipping process may result in the formation of more than one crystalline phase. The analysis of this ring pattern, which was obtained from the dipped face of a CdSe crystal, is presented in the following table, where the numbers at the head of the columns indicate the card number for that particular substance in the ASTM Powder Data File.

<u>Ring #</u>	<u>d, A</u>	<u>(6-0680)</u> <u>Cu<sub>2-x</sub>Se</u>	<u>(4-0839)</u> <u>α-Cu<sub>2</sub>Se</u>	<u>(12-115)</u> <u>CuSe<sub>2</sub></u>	<u>(8-279)</u> <u>Cu<sub>3</sub>Se<sub>2</sub></u>
1	3.33	3.33			
2	3.07			3.083	3.11
3	2.38				2.38
4	1.90			1.904	1.908
5	1.68			1.696	
6	1.26				1.256
7	1.12		1.13		
8	0.968	0.969		0.969	
9	0.929			0.929	

#### GENERAL SUMMARY OF RESULTS AND OBSERVATIONS

- (1) A total of 41 photovoltaic cells were prepared during this period. Of these, 18 were of conducting CdS, 15 were of intermediate resistivity CdS, 5 were of conducting CdSe, and 3 were of ZnS annealed in excess zinc.
- (2) CdSe cells in general give much lower output photovoltage and higher junction capacitance than the CdS cells.
- (3) The ZnS cells generally have very low output and very slow response.
- (4) Cells made with the intermediate resistivity CdS have open-circuit photovoltages comparable to those of conducting CdS, but their output current (and power) is much lower.
- (5) Distortion of the reverse V-I characteristics of intermediate resistivity CdS cells under illumination is thought to be associated with photoconductivity in the CdS.
- (6) Certain intermediate CdS cells show an increase in frontwall open-

circuit photovoltage when light of wavelength less than 7000 Å is blocked out.

- (7) CdS cells made by dipping in a solution of  $\text{Cu}_2\text{S} + \text{NH}_4\text{OH}$  have spectral response curves which fall off rapidly for wavelengths greater than 5000 Å, whereas those dipped in the  $\text{CuCl}$  solution generally exhibit a plateau which extends out to about 9000 Å.
- (8) Cell parameters tend to improve with heat treatment up to some maximum, and then decrease with increasing time of heating.
- (9) CdS single crystals cleave readily on  $(11\bar{2}0)$ ; the cleaved surfaces react more slowly with the  $\text{CuCl}$  solution than do etched or ground surfaces.
- (10) Measurements of the junction capacitance of CdS cells show significant differences from the usual voltage dependence of the capacitance of p-n junctions. There appears to be a relationship between the shape of the C-V plot and the I-V characteristic.
- (11) Transient effects accompany capacitance measurements on CdS cells when (a) a reverse bias is suddenly applied, or (b) the illumination is suddenly changed.
- (12) Electron diffraction evidence indicates that polycrystalline, and sometimes polyphase, layers are formed by the  $\text{CuCl}$  dipping process. Longer dipping times than those used in the experiments thus far may be required to promote the epitaxial relation with the substrate recently reported in the literature.
- (13) For all the intermediate resistivity CdS cells tested, the effect of 9000 Å bias light, if any, is to decrease the photovoltage at wavelengths shorter than the band edge of CdS, sometimes to zero.



- (14) For the conducting CdS cells, the effect of the 9000 Å bias light is to increase the photovoltage for  $\lambda < 7000 \text{ \AA}$ , and decrease it slightly for longer wavelengths. (This statement is made with reference to cells processed in air).
- (15) The most effective wavelength of bias illumination appears to be 9000 Å. No effect has yet been observed for a bias light wavelength of 5000 Å.

#### FUTURE EXPERIMENTS

The experiments performed during the report period just completed have shown the general type of results to be expected from single-crystal II-VI photovoltaic cells produced by the dipping method. During the next period, a limited number of much more carefully designed experiments will be initiated.

The first step will be to grow some large single crystals of CdS, both undoped and doped, by the moving-temperature-gradient method, and to characterize these crystals by the measurement of their electronic and structural properties. The next step will be to process these crystals to form photovoltaic cells in a systematic and carefully controlled manner. Facilities for performing chemical dipping and heat treating in inert atmosphere are being set up.

In addition to the "standard" photocell measurements described in this report, some specialized experiments involving a light microprobe are being planned in order to help answer the fundamental question regarding the location of the light absorption. It is also planned to explore the effect of temperature on photocell performance.

Experiments involving chemically sprayed  $\text{Cu}_2\text{S}$  layers on CdS and

CdSe crystals, and  $\text{Cu}_2\text{Se}$  layers on CdS and CdSe crystals, are also anticipated.

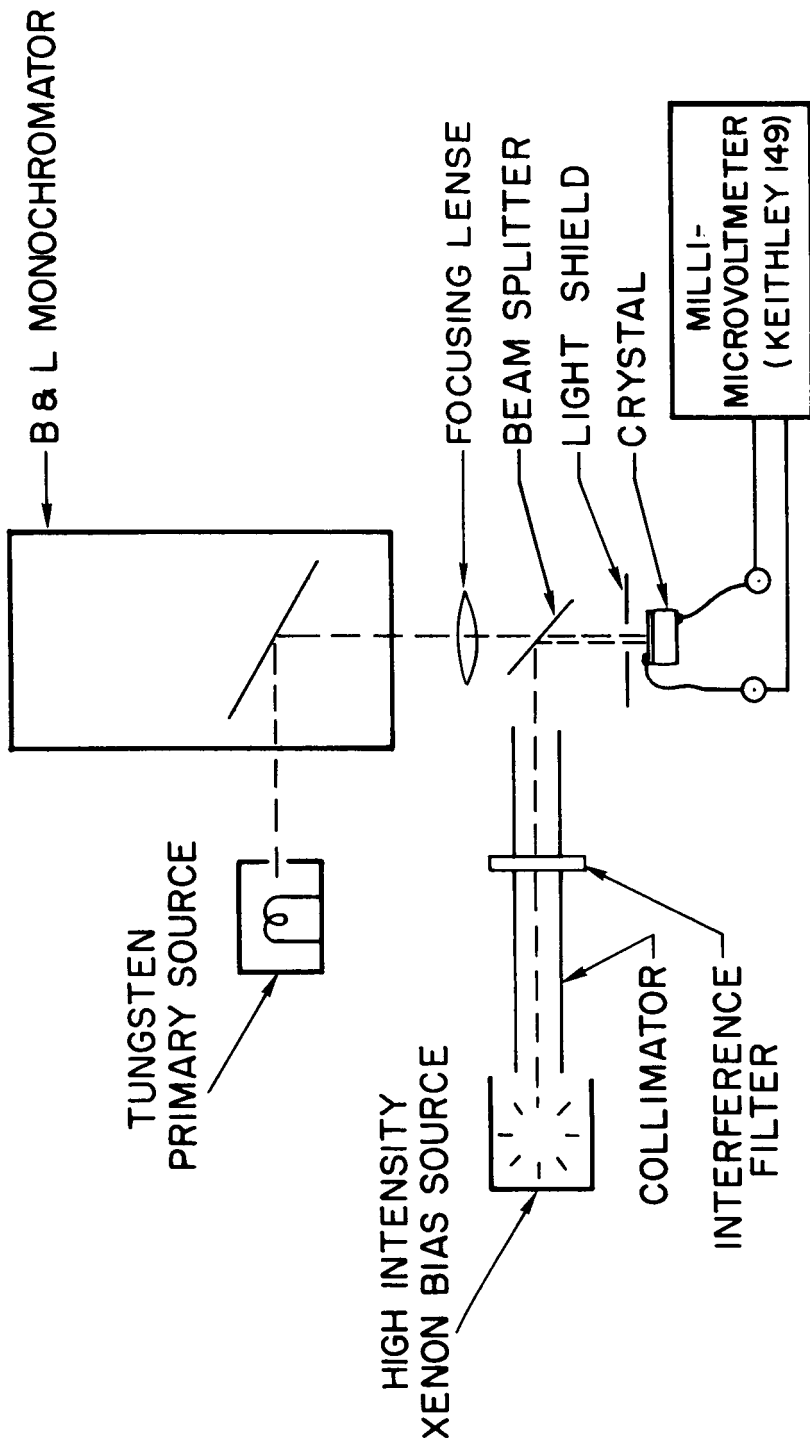
#### REFERENCES

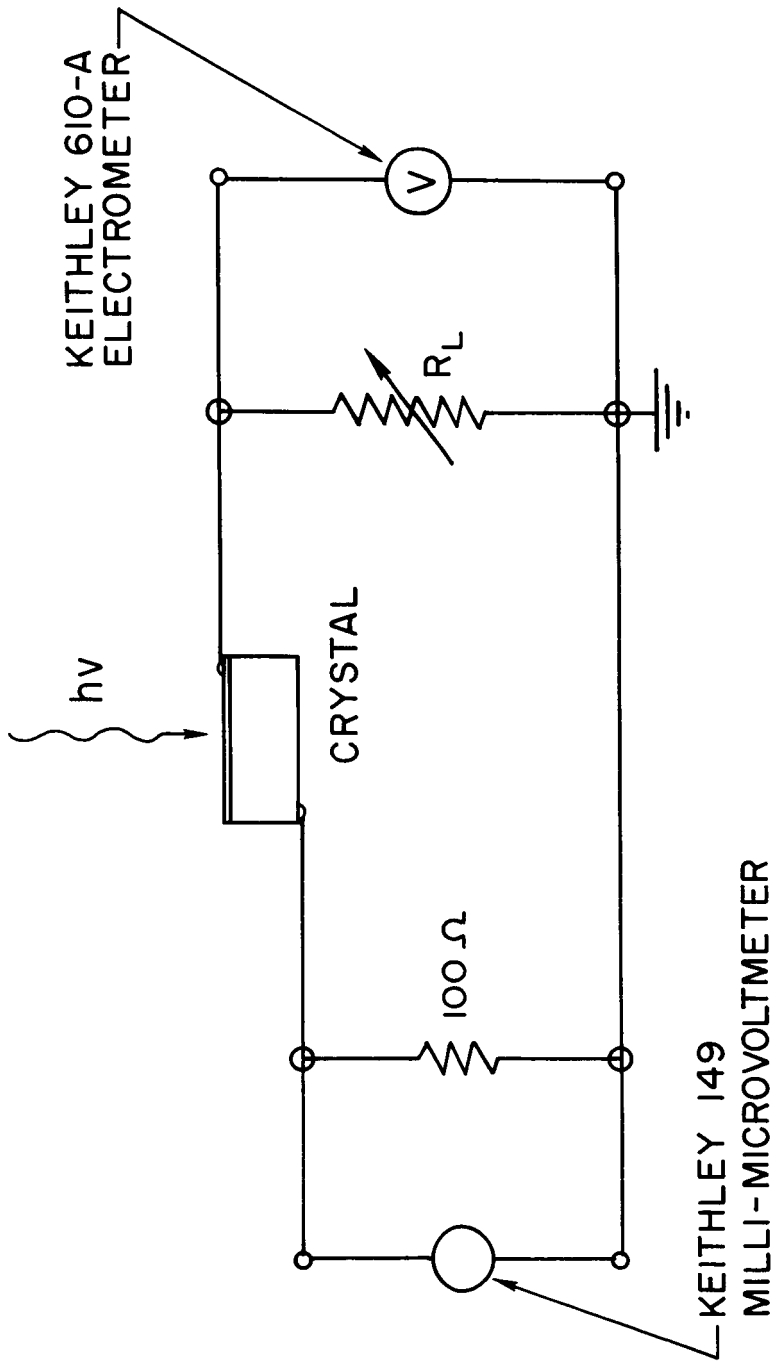
1. L. R. Shiozawa, G. A. Sullivan, and F. Augustine, "Research on the Mechanism of the Photovoltaic Effect in High Efficiency CdS Thin Film Solar Cells", Interim Technical Report #1, Electronic Research Division, Clevite Corporation, July, 1967.
2. Y. Furukawa, and Y. Ishibashi, Review of the Electrical Communication Laboratory 15, 78 (1967).
3. J. Singer and P. A. Faeth, Appl. Phys. Letters 11, 130 (1967).

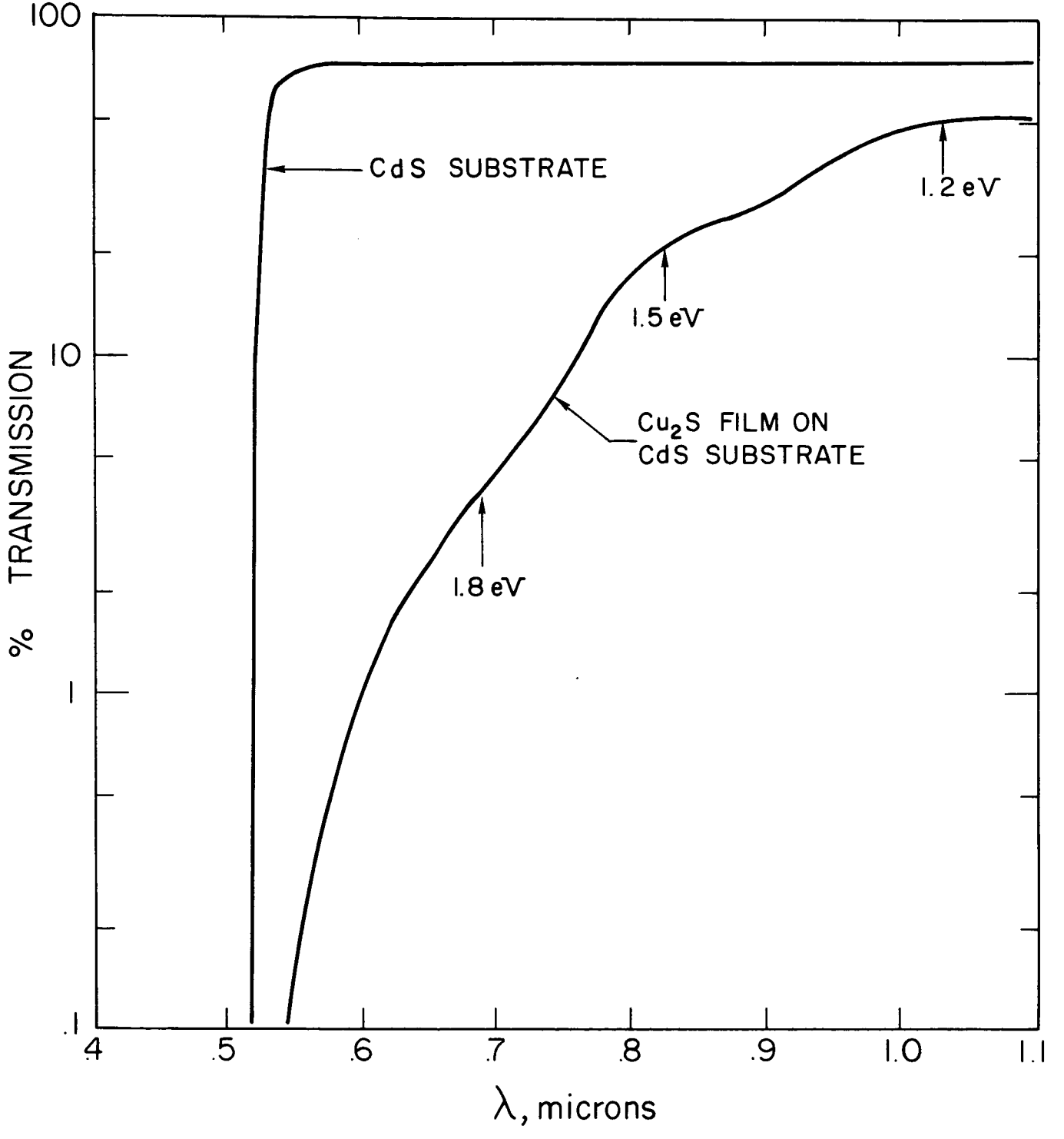
### FIGURE CAPTIONS

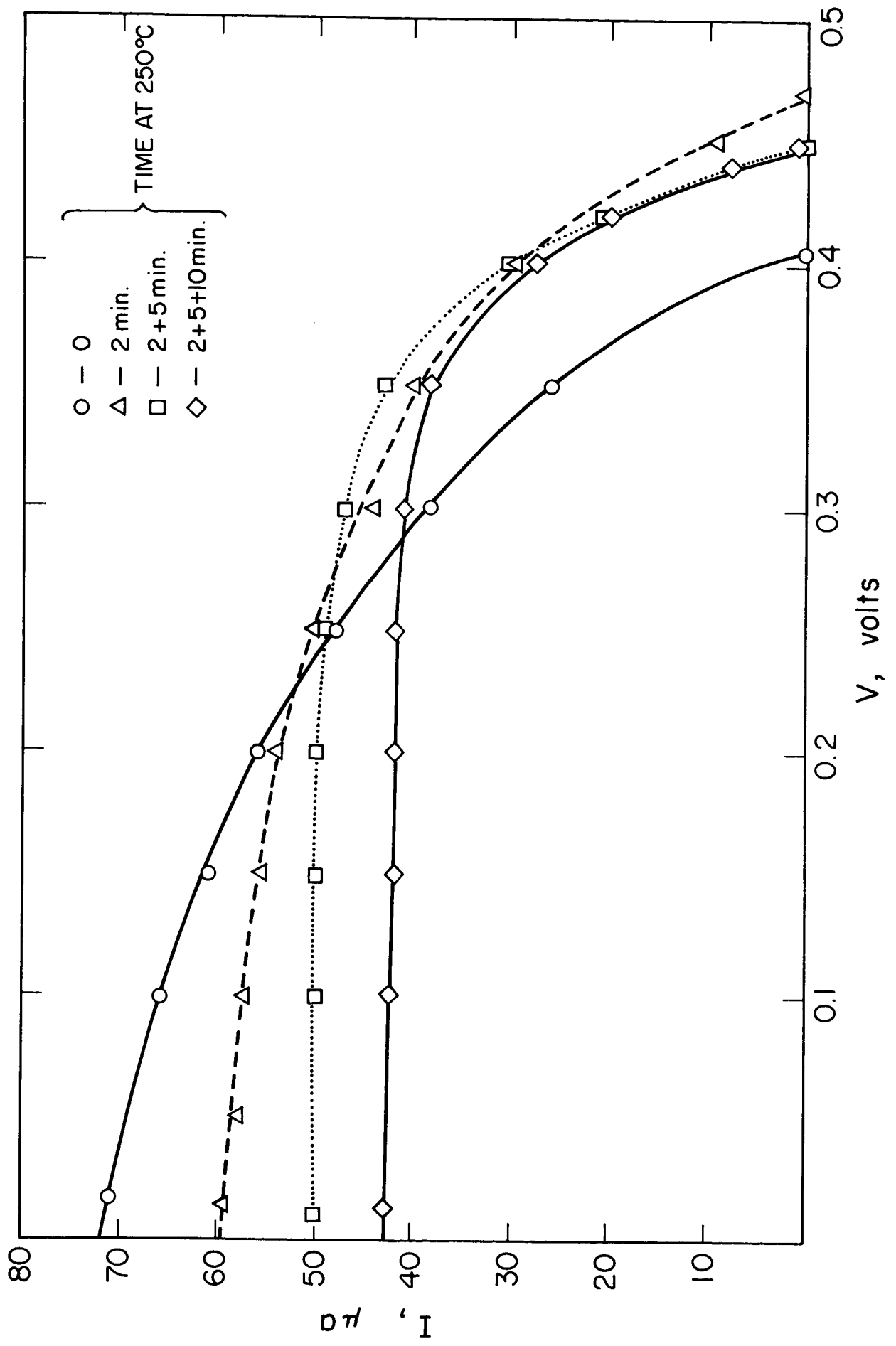
- Fig. 1 Experimental arrangement for measurement of spectral response of photovoltaic cells.
- Fig. 2 Circuit used for power measurements on photovoltaic cells.
- Fig. 3 Per cent transmission as a function of wavelength for single crystal CdS substrate, and substrate with dipped  $\text{Cu}_2\text{S}$  layer.
- Fig. 4 Power as a function of time at  $250^\circ\text{C}$  in air for CdS photocell with cleaved face dipped in  $\text{CuCl}$  solution.
- Fig. 5 V-I characteristic of CdS cell of Fig. 4, after 17 minutes heat treatment at  $250^\circ\text{C}$ .
- Fig. 6 Frontwall spectral response of same CdS cell, with and without  $9000 \text{ \AA}$  bias light.
- Fig. 7 Frontwall spectral response of another CdS cell, showing larger effect of  $9000 \text{ \AA}$  bias light.
- Fig. 8 V-I characteristic of intermediate resistivity CdS cell: (a) in dark (b) with white illumination, backwall.
- Fig. 9 Frontwall spectral response of intermediate resistivity CdS cell showing large negative effect of  $9000 \text{ \AA}$  bias light.
- Fig. 10 Forward V-I characteristic of CdS cell formed by dipping in solution of  $\text{Cu}_2\text{S}$  in  $\text{NH}_4\text{OH}$ .
- Fig. 11 Frontwall and backwall spectral response of same cell.
- Fig. 12 Capacitance-voltage plot for CdS cell dipped in  $\text{Cu}_2\text{S}$  solution.
- Fig. 13 Decay of zero-bias capacitance with time after shutting off white light. Same cell as Fig. 10-12.
- Fig. 14 Change of capacitance with time after application of 1.0 volt reverse bias. Same cell as Fig. 13.

- Fig. 15 Fit of data of Fig. 14 to exponential function.
- Fig. 16 Debye-Scherrer X-ray film of piece of dipped layer from CdS crystal. Exposure was 6 hours in  $\text{CuK}\alpha$  radiation.
- Fig. 17 Reflection electron diffraction pattern of dipped layer on CdS crystal. Pattern is indexed as  $\text{Cu}_2\text{S}$  in the  $[2\bar{1}\bar{3}]$  orientation.
- Fig. 18 Reflection electron diffraction pattern of dipped layer on CdS crystal, indicating the presence of several copper selenide phases.

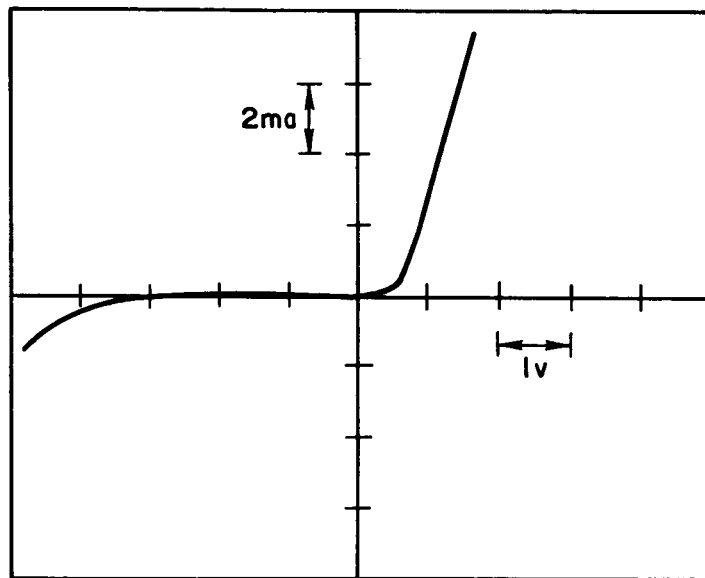


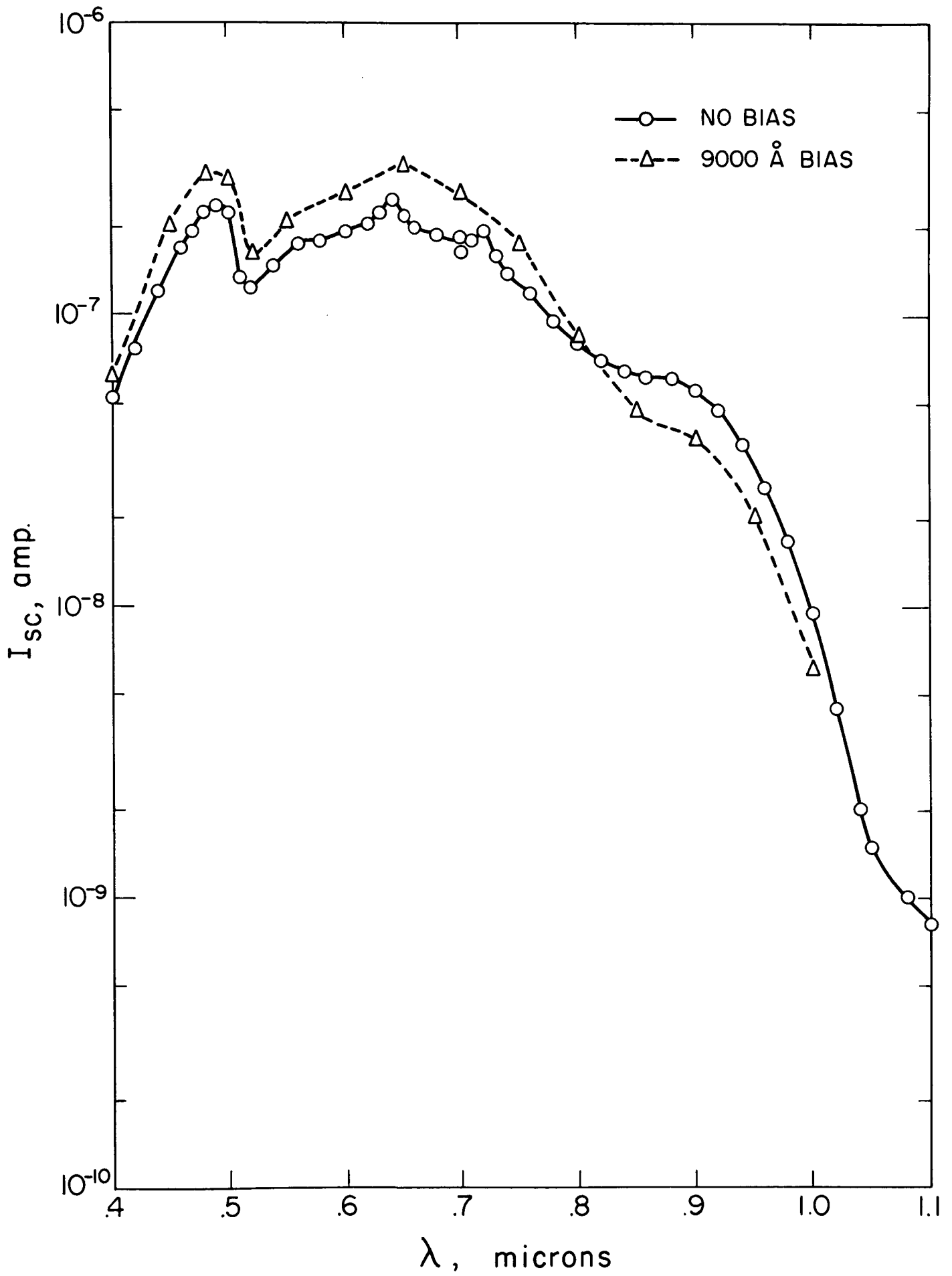


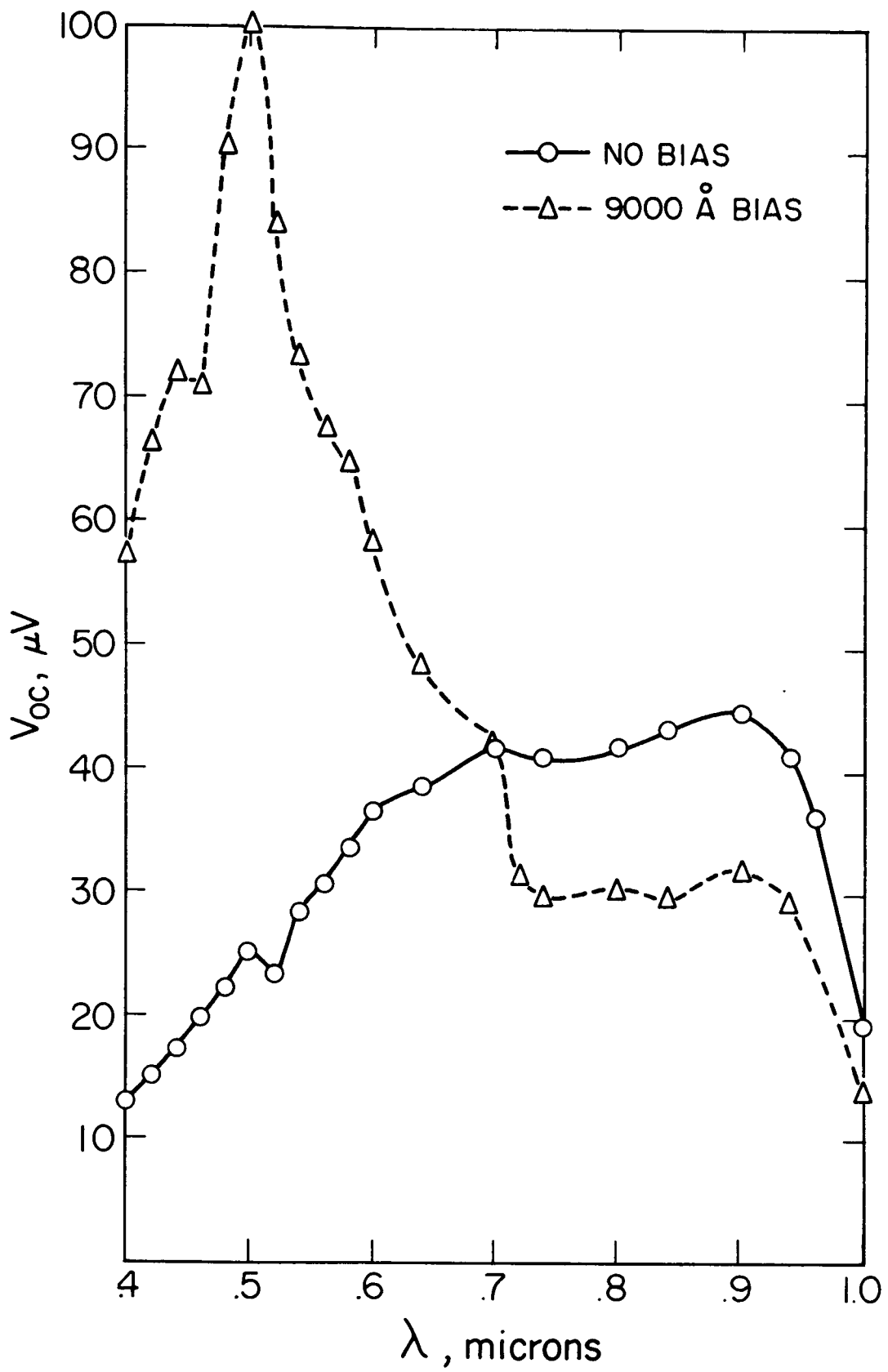


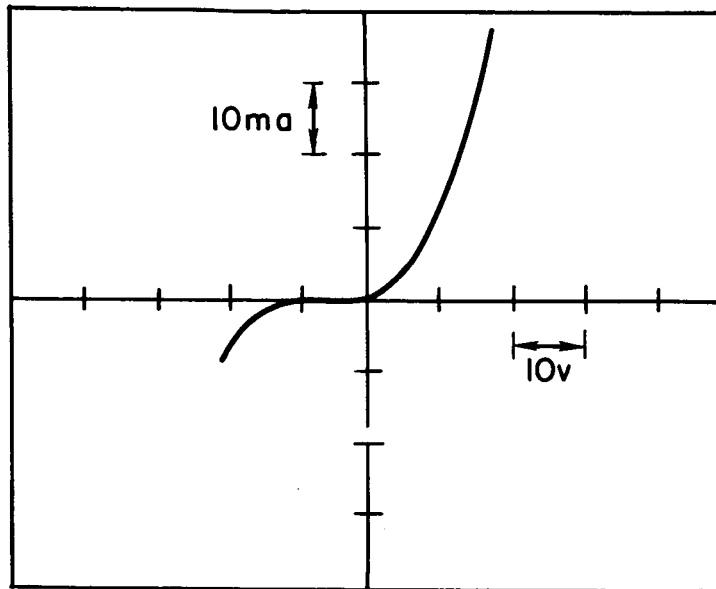




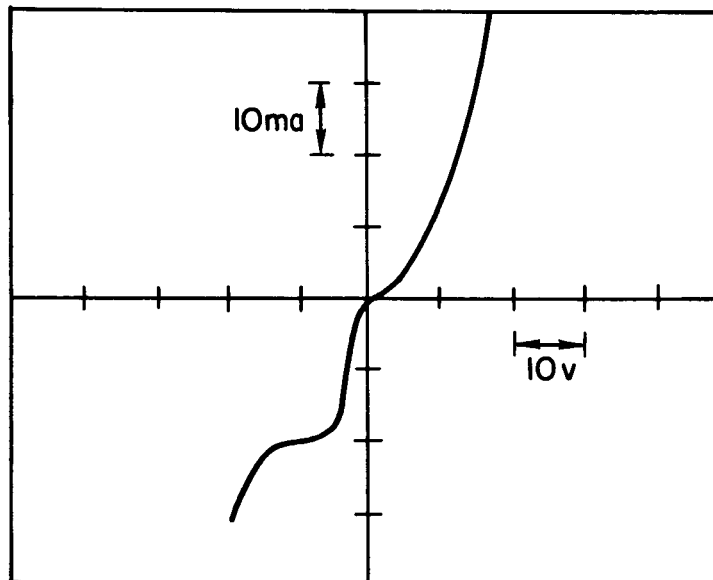








(a) DARK



(b) WHITE ILLUMINATION BACKWALL

